

Mechanistic Diversity Covering 15 Orders of Magnitude in Rates: Cyanide Exchange on $[M(CN)_4]^{2-}$ ($M = Ni, Pd, \text{ and } Pt$)¹

Florence J. Monlien, Lothar Helm, Amira Abou-Hamdan, and André E. Merbach*

Contribution from the Institut de Chimie Moléculaire et Biologique, Ecole Polytechnique Fédérale de Lausanne, EPFL-BCH, CH-1015 Lausanne, Switzerland

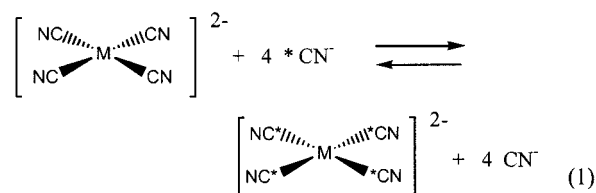
Received August 20, 2001

Kinetic studies of cyanide exchange on $[M(CN)_4]^{2-}$ square-planar complexes ($M = Pt, Pd, \text{ and } Ni$) were performed as a function of pH by ¹³C NMR. The $[Pt(CN)_4]^{2-}$ complex has a purely second-order rate law, with CN^- as acting as the nucleophile, with the following kinetic parameters: $(k_2^{Pt,CN})^{298} = 11 \pm 1 \text{ s}^{-1} \text{ mol}^{-1} \text{ kg}$, $\Delta H_2^\ddagger Pt,CN = 25.1 \pm 1 \text{ kJ mol}^{-1}$, $\Delta S_2^\ddagger Pt,CN = -142 \pm 4 \text{ J mol}^{-1} \text{ K}^{-1}$, and $\Delta V_2^\ddagger Pt,CN = -27 \pm 2 \text{ cm}^3 \text{ mol}^{-1}$. The Pd(II) metal center has the same behavior down to pH 6. The kinetic parameters are as follows: $(k_2^{Pd,CN})^{298} = 82 \pm 2 \text{ s}^{-1} \text{ mol}^{-1} \text{ kg}$, $\Delta H_2^\ddagger Pd,CN = 23.5 \pm 1 \text{ kJ mol}^{-1}$, $\Delta S_2^\ddagger Pd,CN = -129 \pm 5 \text{ J mol}^{-1} \text{ K}^{-1}$, and $\Delta V_2^\ddagger Pd,CN = -22 \pm 2 \text{ cm}^3 \text{ mol}^{-1}$. At low pH, the tetracyanopalladate is protonated ($pK_a^{Pd(4,H)} = 3.0 \pm 0.3$) to form $[Pd(CN)_3HCN]^-$. The rate law of the cyanide exchange on the protonated complex is also purely second order, with $(k_2^{PdH,CN})^{298} = (4.5 \pm 1.3) \times 10^3 \text{ s}^{-1} \text{ mol}^{-1} \text{ kg}$. $[Ni(CN)_4]^{2-}$ is involved in various equilibrium reactions, such as the formation of $[Ni(CN)_5]^{3-}$, $[Ni(CN)_3HCN]^-$, and $[Ni(CN)_2(HCN)_2]$ complexes. Our ¹³C NMR measurements have allowed us to determine that the rate constant leading to the formation of $[Ni(CN)_5]^{3-}$ is $k_2^{Ni(4),CN} = (2.3 \pm 0.1) \times 10^6 \text{ s}^{-1} \text{ mol}^{-1} \text{ kg}$ when the following activation parameters are used: $\Delta H_2^\ddagger Ni,CN = 21.6 \pm 1 \text{ kJ mol}^{-1}$, $\Delta S_2^\ddagger Ni,CN = -51 \pm 7 \text{ J mol}^{-1} \text{ K}^{-1}$, and $\Delta V_2^\ddagger Ni,CN = -19 \pm 2 \text{ cm}^3 \text{ mol}^{-1}$. The rate constant of the back reaction is $k_{-2}^{Ni(4),CN} = 14 \times 10^6 \text{ s}^{-1}$. The rate law pertaining to $[Ni(CN)_2(HCN)_2]$ was found to be second order at pH 3.8, and the value of the rate constant is $(k_2^{Ni(4,2H),CN})^{298} = (63 \pm 15) \times 10^6 \text{ s}^{-1} \text{ mol}^{-1} \text{ kg}$ when $\Delta H_2^\ddagger Ni(4,2H),CN = 47.3 \pm 1 \text{ kJ mol}^{-1}$, $\Delta S_2^\ddagger Ni(4,2H),CN = 63 \pm 3 \text{ J mol}^{-1} \text{ K}^{-1}$, and $\Delta V_2^\ddagger Ni(4,2H),CN = -6 \pm 1 \text{ cm}^3 \text{ mol}^{-1}$. The cyanide-exchange rate constant on $[M(CN)_4]^{2-}$ for Pt, Pd, and Ni increases in a 1:7:200 000 ratio. This trend is modified at low pH, and the palladium becomes 400 times more reactive than the platinum because of the formation of $[Pd(CN)_3HCN]^-$. For all cyanide exchanges on tetracyano complexes (A mechanism) and on their protonated forms (II_a mechanisms), we have always observed a pure second-order rate law: first order for the complex and first order for CN^- . The nucleophilic attack by HCN or solvation by H₂O is at least nine or six orders of magnitude slower, respectively than is nucleophilic attack by CN^- for Pt(II), Pd(II), and Ni(II), respectively.

Introduction

We have investigated the kinetics of oxygen and cyanide exchange on the dioxotetracyanometalate complexes of Os(VI), Re(V), Tc(V), W(IV), and Mo(IV).³ We now extend this study to cyanide exchange on the tetracyanometalate complexes $[M(CN)_4]^{2-}$ ($M = Ni, Pd \text{ and } Pt$) that are thermodynamically stable yet kinetically labile in water.⁴ These square-planar tetracyano complexes provide us with

a rare example of a mechanistic study (eq 1) that can be performed on the same Pt(II), Pd(II), and Ni(II) complexes.



The reactions involving the displacement of ligands in square-planar d⁸ transition-metal complexes can be described

* Corresponding author. E-mail: andre.merbach@epfl.ch.

(1) Part 98 of the series on high-pressure NMR kinetics.

(2) Monlien, F. J.; Helm, L.; Abou-Hamdan, A.; Merbach, A. E. *Inorg. Chim. Acta*. In press (part 97 of the series on high-pressure NMR kinetics).

by the two-term equation⁵ $k_{\text{obs}} = k_1 + k_2 [\text{ligand}]$. The second-order rate constant k_2 refers to a direct attack of the ligand on the substrate, and the pseudo-first-order rate constant k_1 , to the attack of the solvent. The value of the k_1 term depends only on the nature the solvent. The square-planar complexes have characteristic kinetic behavior involving a five-coordinate intermediate or transition state. Early exchange studies^{6,7} with heavy-metal cyanide complexes were monitored with counting techniques using ¹⁴C-labeled radiocyanide. Today, the rate of cyanide exchange is accessible by kinetic NMR methods and by preliminary results of the exchange on Pt(II) and Pd(II) for pH = 10.3–10.8.⁸ The rate law was found to be second order, and no cyanide-independent pathway was observed. Under these conditions, the cyanide exchange for $[\text{Ni}(\text{CN})_4]^{2-}$ was found to be too fast on the NMR time scale to be determined.

We have extended the ¹³C NMR study to the cyanide exchange from pH = 1–12.5 to determine if HCN or H₂O can act as nucleophiles. Because of the large numerical range of the rate constants, kinetic studies were monitored by line-broadening using the Kubo–Sack formalism as well as magnetization-transfer and isotopic-labeling techniques. Variable pressure experiments were performed to assign the cyanide exchange mechanism to these metal centers. The variation of the pH leads to mechanistic diversity involving pentacoordinated species and protonation of the tetracyano-complexes.

Experimental Section

Materials and Solutions. $\text{K}_2[\text{Pt}(\text{CN})_4] \cdot 3\text{H}_2\text{O}$, $\text{K}_2[\text{Pd}(\text{CN})_4] \cdot 3\text{H}_2\text{O}$, and $\text{K}_2[\text{Ni}(\text{CN})_4] \cdot \text{H}_2\text{O}$ (Aldrich) and K^{13}CN (Cambridge isotope laboratory, 99% enriched) were of the highest quality available (p.a.) and were used without further purification. Aqueous solutions of about 0.1 mol kg⁻¹ of each complex with variable concentrations of KCN were freshly prepared before each experiment. The ionic strength of each solution was fixed to 0.65 ± 0.10 mol kg⁻¹ by adding KNO_3 or KCF_3SO_3 . The pH was adjusted by adding concentrated HNO_3 or $\text{CF}_3\text{SO}_3\text{H}$ and KOH.

pH Measurements. pH values were determined by the potentiometric technique using a titroprocessor (Titrino 716 from Metrohm) for the addition of titrant and for mV readings. A combined glass/reference electrode with a symmetrical electrode chain (Radiometer Analytical S. A., pHc2406L) and a Metrohm 713 pH meter were calibrated from titrations of HCl with NaOH

at $T = 298.1$ K and $I = 0.60$ mol kg⁻¹. If the pH differed by more than 0.1 unit between the beginning and the end of an NMR measurement, the data were not accepted.

NMR Measurements. NMR spectra were recorded with Bruker DPX-400 and ARX-400 spectrometers. All solutions used for ¹³C measurements contained 2% D₂O as the internal lock substance and ¹³CH₃OH as an internal chemical shift reference (49.3 ppm with respect to TMS). Methanol was also used as reference for B_0 homogeneity. The temperature was controlled by a Bruker B-VT 3000 unit and measured by substituting the sample tube for one containing a platinum Pt-100 resistor (accuracy = 0.5 K).⁹ Slow isotopic-exchange kinetics were followed after mixing two thermostated solutions at the same pH using a fast injection unit¹⁰ or manual injection. The mixing time was less than 0.5 s. The number of spectra (15–50), the number of scans for each spectrum, and the supplementary delay between two successive spectra were adjusted according to the rate of the exchange reaction.

Magnetization transfer measurements were performed using the “inversion recovery technique” as described in the literature.¹¹ This technique can be performed when the longitudinal relaxation rate $1/T_1$ is less than or equal to the exchange rate. The exchange rate between two sites can be deduced by selectively inverting the signal of one and by monitoring the intensity of the signals at both sites as a function of the delay τ between the perturbation and the acquisition pulses. Selective inversion of the bound or free signal was achieved using the so-called “1–3–3–1” pulse train.¹² The return of the magnetization to equilibrium is then governed by both the $1/T_1$ value of the exchanging species and the exchange rate between the sites.¹³

High-pressure high-resolution NMR spectra were monitored with a home-built narrow bore probe (5 mm NMR tube).¹⁴ Tetrachloroethylene (above 298 K) and Fluobrene (below 298 K) were used as pressurization liquids. By pumping a thermostated liquid (synthetic oil above 298 K and ethanol below 298 K) through the high-pressure vessel, the temperature was stabilized to ± 0.2 K. The experiments were performed between 273.1 and 353.1 K.

Programs. Line widths of NMR signals were obtained by fitting Lorentzian functions to the experimental spectra using the *NM-RICMA 2.7* program¹⁵ for Matlab.¹⁶ The adjustable parameters are the resonance frequency, intensity, line width, baseline, and phasing. Complete line-shape analysis based on the Kubo–Sack formalism using modified Bloch equations was also performed with *NM-RICMA 2.7* to extract rate constants from experimental spectra. Data analysis was carried out with the nonlinear least-squares fitting program *Scientist*.¹⁷ The reported errors correspond to 1σ .

Results

Cyanide Exchange on $[\text{M}(\text{CN})_4]^{2-}$ as a Function of pH. Cyanide exchange on Pt(II), Pd(II), and Ni(II) was studied

- (3) (a) Roodt, A.; Leipoldt, J. G.; Helm, L.; Merbach, A. E. *Inorg. Chem.* **1992**, *31*, 2864. (b) Roodt, A.; Leipoldt, J. G.; Helm, L.; Merbach, A. E. *Inorg. Chem.* **1994**, *33*, 140. (c) Roodt, A.; Leipoldt, J. G.; Helm, L.; Abou-Hamdan, A.; Merbach, A. E. *Inorg. Chem.* **1995**, *34*, 560. (d) Abou-Hamdan, A.; Roodt, A.; Merbach, A. E. *Inorg. Chem.* **1998**, *37*, 1278. (e) Roodt, A.; Abou-Hamdan, A.; Engelbrecht, H. P.; Merbach, A. E. *Adv. Inorg. Chem.* **2000**, *49*, 59.
- (4) Sharpe, A. G. *The Chemistry of Cyano Complexes of the Transition Metals*; Academic Press: New York, 1976.
- (5) (a) Lincoln, S. F.; Merbach, A. E. *Adv. Inorg. Chem.*; Sykes, A. G.; Academic Press: 1995, 1; (b) Tobe, M. L.; Burgess, J. *Inorganic Reaction Mechanisms*; Longman Group: Harlow, U.K., 1999. (c) Basolo, F.; Pearson, R. G. *Mechanism of Inorganic Reactions*, 2nd ed; Wiley & Sons: New York, 1965. (d) Cross, R. J. *Adv. Inorg. Chem.* **1989**, *34*, 219.
- (6) Adamson, A. W.; Welker, J. P.; Volpe, M. *J. Am. Chem. Soc.* **1950**, *73*, 4030.
- (7) Long, F. A. *J. Am. Chem. Soc.* **1951**, *78*, 537.
- (8) Pesek, J. J.; Mason, W. R. *Inorg. Chem.* **1983**, *22*, 2958.

- (9) Ammann, C.; Meier, P.; Merbach, A. E. *J. Magn. Reson.* **1982**, *46*, 319.
- (10) Bernhard, P.; Helm, L.; Ludi, A.; Merbach, A. E. *J. Am. Chem. Soc.* **1985**, *107*, 312.
- (11) (a) Dahlquist, F. W.; Longmuir, K. J.; Du Vernet, R. B. *J. Magn. Reson.* **1975**, *17*, 406. (b) Alger, J. R.; Prestegord, J. H. *J. Magn. Reson.* **1977**, *27*, 137. (c) Led, J. J.; Gesmar, H. *J. Magn. Reson.* **1982**, *49*, 444.
- (12) Hore, P. J. *J. Magn. Reson.* **1983**, *55*, 283.
- (13) (a) Led, J. J.; Gesmar, H. *J. Magn. Reson.* **1982**, *49*, 444. (b) Mann, B. E. *Annu. Rep. NMR Spectrosc.* **1982**, *12*, 263.
- (14) (a) Cusanelli, A.; Nicula-dadci, L.; Frey, U.; Merbach, A. E. *Inorg. Chem.* **1997**, *36*, 2211. (b) Frey, U.; Helm, L.; Merbach, A. E.; Roulet, R. *Advanced Applications of NMR to Organometallic Chemistry*; Wiley & Sons: New York, 1996.
- (15) Helm, L.; Borel, A. *NM-RICMA 2.7*; University of Lausanne: 2000.
- (16) *Matlab*, version 5.3.1; Mathworks Inc.: 1999.
- (17) *Scientist*, version 2.0; Micromath, Inc.: Salt Lake City, UT, 1995.

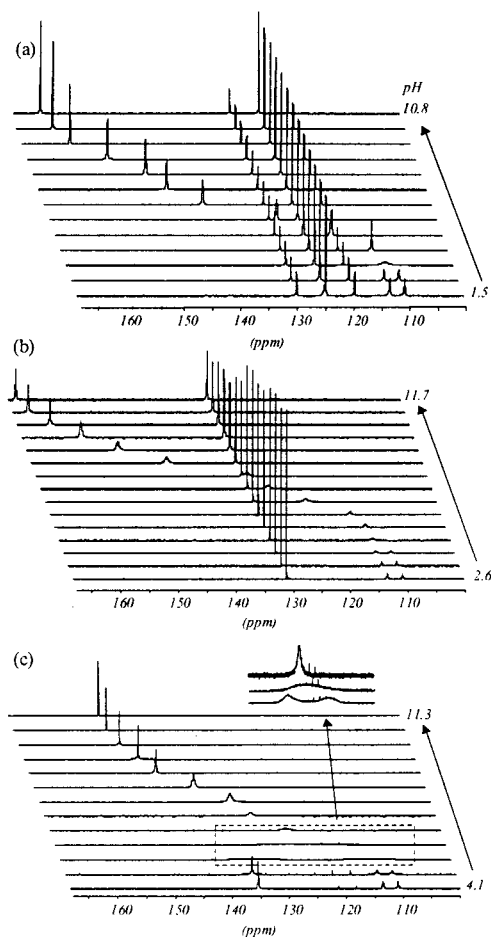


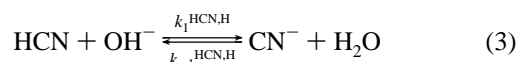
Figure 1. ^{13}C NMR spectra measured as a function of pH at 298.1 K ($\text{D}_2\text{O}/\text{H}_2\text{O} = 2\%$) for solutions containing 0.1 mol kg^{-1} of $\text{K}_2[\text{M}(\text{CN})_4]$ and 0.4 mol kg^{-1} K^{13}CN . (a) $\text{M} = \text{Pt}(\text{II})$. (b) $\text{M} = \text{Pd}(\text{II})$. (c) $\text{M} = \text{Ni}(\text{II})$.

at $T = 298.1 \text{ K}$ as a function of pH using ^{13}C NMR for solutions containing 0.1 mol kg^{-1} of complexes and 0.4 mol kg^{-1} of free cyanide (KCN). The pH profiles are shown in Figure 1. The signal of the $\text{Pt}(\text{II})$ complex is composed of a central line (125.0 ppm) with two satellite lines that are due to cyanide that is bound to the ^{195}Pt isotope with spin $1/2$ ($^1J_{\text{Cpt}} = 1030 \text{ Hz}$). The satellite integral represents 33.8% of the total integrated signal, and the central line, 66.2%. The resonance frequency and the line shape of the complexed ligand are not affected by exchange with free cyanide over the entire pH domain. At low pH, the free ligand is protonated ($\text{p}K_a^{\text{HCN}} = 9.5$). The spectrum of HCN shows a doublet (112.4 ppm) with a coupling constant of $^1J_{\text{CH}} = 272 \text{ Hz}$. With increasing pH, the two doublet signals broaden and coalesce (at pH 7) because of the decreasing lifetime of H^+ on HCN . From pH 8 to 9.5, the coalesced signal broadens and moves toward the CN^- frequency (165.1 ppm), and then the line narrows at basic pH when CN^- predominates.

In Figure 1b, the ^{13}C NMR spectra show a pH-independent resonance frequency of the palladium complex $[\text{Pd}(\text{CN})_4]^{2-}$ (131.2 ppm). Its line width is affected by cyanide exchange only for $\text{pH} > 9$, with a small amount of line broadening. The free ligand shows the same behavior with pH as does the platinum complex; however, the free-ligand line width is slightly affected by the cyanide exchange at basic pH.

The ^{13}C NMR spectrum of the solution containing $\text{K}_2[\text{Ni}(\text{CN})_4]$ and KCN is shown in Figure 1c. At low pH, the HCN (112.4 ppm) and $[\text{Ni}(\text{CN})_4]^{2-}$ (135.5 ppm) signals are broad because of cyanide exchange. These lines broaden when the pH increases, and the signals coalesce at pH 8. The single signal at pH 8 sharpens, and its resonance frequency moves downfield because of the deprotonation of the ligand. Below pH 4, it is not possible to monitor the spectrum because of decomposition and precipitation of the substrate.

Proton Exchange on HCN. The kinetics of the proton exchange on HCN have been reported.^{2,19} For clarity, the three proposed reaction pathways are shown (eqs 2–4).



By combining the rate constants $k_0^{\text{HCN,H}}$, $k_1^{\text{HCN,H}}$, and $k_2^{\text{HCN,H}}$ of the three pathways, the overall rate law for the proton exchange on HCN , $k_{\text{obs}}^{\text{HCN,H}}$, was determined as a function of pH (eq 5). This determination led to the following parameters at 298.1 K: $(k_0^{\text{HCN,H}})^{298} = 113 \pm 17 \text{ s}^{-1}$, $\Delta H_0^\ddagger = 38 \pm 2 \text{ kJ mol}^{-1} \text{ kg}$, $\Delta S_0^\ddagger = -80 \pm 6 \text{ J mol}^{-1} \text{ kg K}^{-1}$, $(k_1^{\text{HCN,H}})^{298} = (2.85 \pm 0.7) \times 10^9 \text{ s}^{-1} \text{ mol}^{-1} \text{ kg}$, and $(k_2^{\text{HCN,H}})^{298} = (0.6 \pm 0.2) \times 10^6 \text{ s}^{-1} \text{ mol}^{-1} \text{ kg}$.

$$k_{\text{obs}}^{\text{HCN,H}} = -\frac{d[\text{HCN}]/[\text{HCN}]}{dt} = \frac{k_0^{\text{HCN,H}} + k_1^{\text{HCN,H}}[\text{OH}^-] + k_2^{\text{HCN,H}}[\text{CN}^-]}{k_0^{\text{HCN,H}} + k_1^{\text{HCN,H}}[\text{OH}^-] + k_2^{\text{HCN,H}}[\text{CN}^-]} \quad (5)$$

Determination of $\text{p}K_a^{\text{HCN}}$. Because of the fast proton exchange on the NMR time scale, the variation of the resonance frequency of the coalesced signal of HCN/CN^- as a function of pH can be used to determine the dissociation constant of HCN , K_a^{HCN} .

$$\delta_{\text{obs}} = \frac{K_a^{\text{HCN}}}{K_a^{\text{HCN}} + [\text{H}^+]} \delta_{\text{CN}^-} + \frac{[\text{H}^+]}{[\text{H}^+] + K_a^{\text{HCN}}} \delta_{\text{HCN}} \quad (6)$$

This NMR titration was performed for solutions containing CN^- and HCN , with and without $[\text{Pt}(\text{CN})_4]^{2-}$ and $[\text{Pd}(\text{CN})_4]^{2-}$. The fitted values for δ_{CN^-} and δ_{HCN} , the resonance frequencies of the CN^- and HCN forms, are 165.1 ± 0.2 and $112.4 \pm 0.2 \text{ ppm}$, respectively, with $\text{p}K_a^{\text{HCN}} = 9.5 \pm 0.2$. The results were the same for all three solutions, within experimental error.

Cyanide Exchange on $[\text{Pt}(\text{CN})_4]^{2-}$. The tetracyanoplatinate(II) complex is very stable in aqueous solution (and even at low pH with excess ligand), with an overall stability constant of $\log \beta_4 = 40$.²⁰ The cyanide-exchange rate law was determined at 298.1 K using pH adjustments to monitor CN^- variation. The exchange rate constants were determined

(18) Bednar, R. A.; Jenks, W. P. *J. Am. Chem. Soc.* **1985**, *107*, 7117.

(19) Banyai, I.; Blixt, J.; Glaser, J.; Toth, I. *Acta Chem. Scand.* **1992**, *46*, 142.

(20) Grinberg, A. A.; Gelman, M. I. *Dokl. Akad. Nauk* **1960**, *133*, 1081.

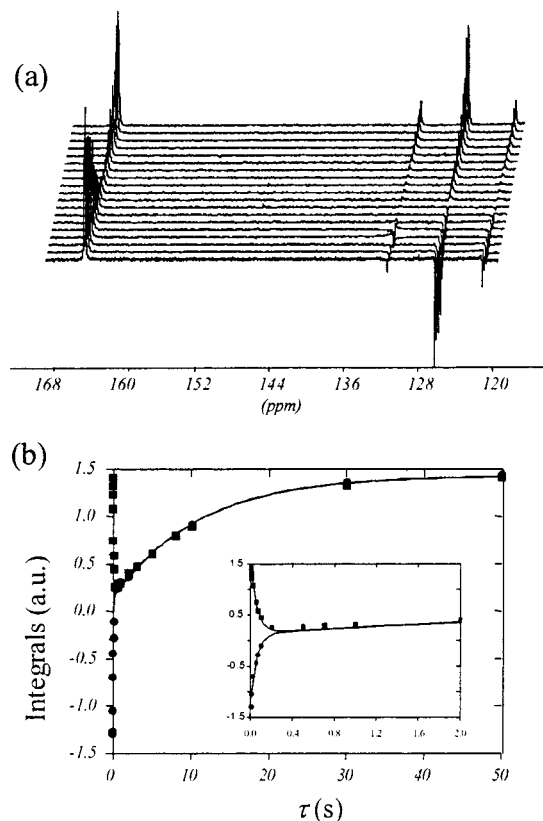


Figure 2. (a) Evolution of high-pressure ^{13}C NMR spectra after selective inversion of the complex signal (125.0 ppm) as a function of the delay between the perturbation and the acquisition pulses at $P = 160$ MPa and $\text{pH} = 11.5$. (b) Least-squares fit of the integrals. $C_{\text{Pt}} = 0.101$ mol kg^{-1} , $C_{\text{CN}} = 0.413$ mol kg^{-1} , $I = 0.69$ mol kg^{-1} , $\text{D}_2\text{O}/\text{H}_2\text{O} = 2\%$, and $T = 298.1$ K.

using the magnetization transfer technique from $\text{pH} 11.7$ to 9.7 . The system includes six sites (one for CN^- , two for HCN because of spin–spin coupling, and three for $[\text{Pt}(\text{CN})_4]^{2-}$) and two exchange processes (for proton exchange on HCN and for cyanide exchange on $[\text{Pt}(\text{CN})_4]^{2-}$). Because of the fast exchange between HCN and CN^- , the signal of the free ligand can be attributed to one unique site. The platinum system is therefore reduced in a two-site complex. Inversion is performed on the three lines of the complex (Figure 2). For each of the spectra collected during the magnetization transfer experiments, Lorentzian functions were fitted to the signals of the free ligand and to the central line as a function of τ . The contribution of the satellite lines to the integral of the central line and the ratio of all the signal line widths were taken into account. The equations given by Led and Gesmar¹³ were fitted to the experimental integrals²¹ using an iterative nonlinear least-squares routine. Nine parameters were adjusted: the final and the initial integrals of the free (f) (CN^-/HCN) and bound (b) ligands, their spin–lattice relaxation rates $1/T_{1f}$ and $1/T_{1b}$, the populations of the two sites, and the exchange rate constant. Below $\text{pH} 8$, magnetization transfer cannot be used; however, at $\text{pH} \leq 6$, the reaction exchange rate is slow enough to be determined using isotopic labeling experiments. The ex-

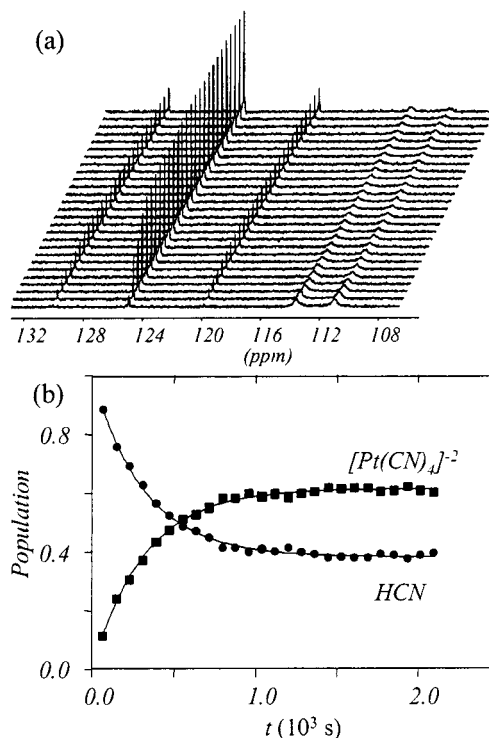


Figure 3. (a) Evolution of ^{13}C NMR spectrum after a rapid mixing of H^{13}CN with $[\text{Pt}(\text{CN})_4]^{2-}$ at $\text{pH} = 6.0$ and 298.1 K. The signal intensity of the complex increases while that of HCN decreases as a function of time. $C_{\text{Pt}} = 0.100$ mol kg^{-1} , $C_{\text{CN}} = 0.262$ mol kg^{-1} , $I = 0.56$ mol kg^{-1} . (b) Time evolution of the ^{13}C populations of HCN and $[\text{Pt}(\text{CN})_4]^{2-}$.

change reactions were followed by rapidly mixing a H^{13}CN solution with a complex solution at the same temperature (298.1 K) and pH using a fast injection unit. We paid special attention to the long relaxation time (T_1) of bound CN^- . Experimental T_1 values as a function of pH for $[\text{Pt}(\text{CN})_4]^{2-}$, HCN/CN^- , and mixtures of $[\text{Pt}(\text{CN})_4]^{2-}$ and HCN/CN^- are from 15 to 22 s. In the presence of cyanide and water containing dissolved O_2 , $[\text{Pt}(\text{CN})_4]^{2-}$ had a shorter ^{13}C relaxation time T_1 than that measured by Pesek et al.²² By monitoring the increase in the intensity of the complex signal and the decrease in the intensity of the free-ligand signal, the kinetics constants were determined with the modified McKay equation (eq 7).^{23,24} A typical example of the $^{13}\text{CN}^-$ signal increase observed with time is given in Figure 3.

$$x(t) = x_{\infty} + (x_0 - x_{\infty}) \exp(-k_{\text{obs}}^{\text{Pt,CN}} t / (1 - x_{\infty})) \quad (7)$$

$x(t)$ represent the mole fraction of coordinated ^{13}CN as a function of time, and x_0 and x_{∞} are the limiting conditions at $t = 0$ and for the exchange equilibrium, respectively. Lorentzian functions were fitted to both NMR signals with *NMRICMA* to determine the values of the integrals as a function of time. $k_{\text{obs}}^{\text{Pt,CN}}$, x_{∞} , and x_0 were determined by fitting the ^{13}C NMR data to eq 7. Isotopic exchange measurements were performed at $\text{pH} 6.0, 3.6, 2.6,$ and 1.1 (Figure 4).

(22) Pesek, J. J.; Mason R. *Inorg. Chem.* **1979**, *18*, 924.

(23) McKay, H. *J. Am. Chem. Soc.* **1943**, *65*, 702.

(24) Lincoln, S. F.; Merbach, A. E. *Adv. Inorg. Chem.*; Sykes A. G., Ed.; Acad. Press: San Diego, 1995.

(21) Frey, U.; Elmroth, S.; Moullet, B.; Elding, L.; Merbach, A. E. *Inorg. Chem.* **1991**, *30*, 5033.

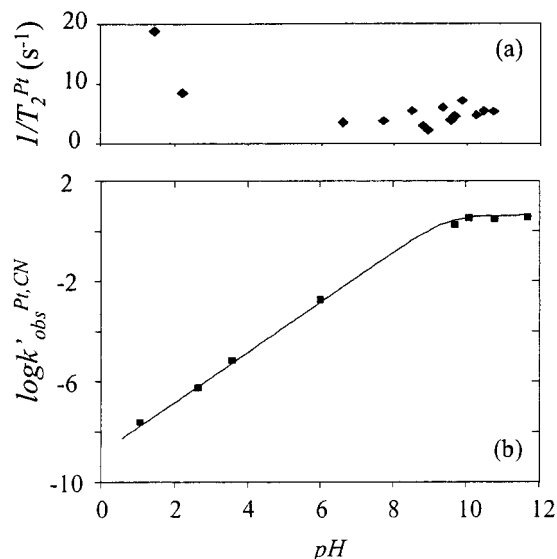


Figure 4. (a) Variation of the ^{13}C NMR line width of the $[\text{Pt}(\text{CN})_4]^{2-}$ signal with pH at 298.1 K. (b) Variation of the concentration-normalized ($C_{\text{CN}} = 0.4 \text{ mol kg}^{-1}$) exchange rate constant $k'_{\text{obs}}^{\text{Pt,CN}}$ with pH for cyanide exchange on $[\text{Pt}(\text{CN})_4]^{2-}$. $C_{\text{Pt}} = 0.100 \text{ mol kg}^{-1}$, $I = 0.69 \text{ mol kg}^{-1}$, $\text{D}_2\text{O}/\text{H}_2\text{O} = 2\%$, and $T = 298.1 \text{ K}$.

Analysis of the pH dependence (eq 8) indicates a purely second-order rate law (Figure 4) with $(k_2^{\text{Pt,CN}})^{298} = 11 \pm 1 \text{ s}^{-1} \text{ mol}^{-1} \text{ kg}$.

$$k_{\text{obs}}^{\text{Pt,CN}} = \frac{-d[\text{Pt}(\text{CN})_4^{2-}]}{dt [\text{Pt}(\text{CN})_4^{2-}]} = k_2^{\text{Pt,CN}} [\text{CN}^-] = k_2^{\text{Pt,CN}} C_{\text{CN}} \frac{K_a^{\text{HCN}}}{K_a^{\text{HCN}} + [\text{H}^+]} \quad (8)$$

where C_{CN} is the analytical concentration of the free cyanide.

A variable-temperature study of the exchange rate constant, $k_{\text{obs}}^{\text{Pt,CN}}$, was performed by ^{13}C NMR magnetization transfer from 271.1 to 317.1 K at pH = 11.5 on a solution containing $0.096 \text{ mol kg}^{-1}$ of the Pt complex and $0.392 \text{ mol kg}^{-1}$ of the free cyanide. Higher temperatures cannot be used because of cyanide decomposition. Fitting eq 9 to the data led to the following activation parameters: $(k_2^{\text{Pt,CN}})^{298} = 11 \pm 1 \text{ s}^{-1} \text{ mol}^{-1} \text{ kg}$, $\Delta H_2^\ddagger^{\text{Pt,CN}} = 25.1 \pm 0.4 \text{ kJ mol}^{-1}$, and $\Delta S_2^\ddagger^{\text{Pt,CN}} = -142 \pm 2 \text{ J mol}^{-1} \text{ K}^{-1}$.

$$k_2^{\text{Pt,CN}} = \frac{k_B T}{h} \exp\left[\frac{\Delta S_2^\ddagger}{R} - \frac{\Delta H_2^\ddagger}{RT}\right] = (k_2^{\text{Pt,CN}})^{298} \frac{T}{298.1} \exp\left[\frac{\Delta H_2^\ddagger}{R} \left(\frac{1}{298.1} - \frac{1}{T}\right)\right] \quad (9)$$

Variable-pressure experiments on ^{13}C NMR magnetization transfer were performed as a function of pressure at pH 11.5 on a solution containing $0.101 \text{ mol kg}^{-1}$ of the Pt complex and $0.413 \text{ mol kg}^{-1}$ of the free cyanide. Equation 10 was fitted (Figure 2) to the exchange rate constant obtained as a function of pressure, leading to the rate constant at zero pressure $(k_2^{\text{Pt,CN}})_0 = 10.2 \pm 0.3 \text{ s}^{-1} \text{ mol}^{-1} \text{ kg}$, the activation volume $\Delta V_2^\ddagger^{\text{Pt,CN}} = -27 \pm 2 \text{ cm}^3 \text{ mol}^{-1}$, and the compress-

ibility coefficient of activation $\Delta\beta^\ddagger = -(10 \pm 2) \times 10^{-2} \text{ cm}^3 \text{ mol}^{-1} \text{ MPa}^{-1}$.

$$k_2^{\text{Pt,CN}} = (k_2^{\text{Pt,CN}})_0 \exp\left(-\frac{\Delta V_2^\ddagger}{RT} P + \frac{\Delta\beta^\ddagger}{2RT} P^2\right) \quad (10)$$

Cyanide Exchange on $[\text{Pd}(\text{CN})_4]^{2-}$. The tetracyanopalladate(II) is also very stable in aqueous solution. Its overall formation constant as determined by Fasman et al. is $\log \beta_4 = 51.7$.²⁵ The rate law of the cyanide exchange on $[\text{Pd}(\text{CN})_4]^{2-}$ was determined at pH = 11.4. ^{13}C NMR spectra of 0.05 mol kg^{-1} $[\text{Pd}(\text{CN})_4]^{2-}$ solutions containing variable KCN concentrations (0.053 – $0.427 \text{ mol kg}^{-1}$) at fixed ionic strength ($I = 0.6 \pm 0.1 \text{ mol kg}^{-1}$) were measured at 298.1 K. The resonance frequencies of the complexed (131.2 ppm) and the free (165.1 ppm) cyanide did not change, whereas their line widths broaden with increasing free-cyanide concentration. The inverse of the mean lifetime of cyanide on $[\text{Pd}(\text{CN})_4]^{2-}$, $1/\tau^{\text{Pd}} = k_r^{\text{Pd}}$, were extracted from the NMR spectra by line-shape analysis using the Kubo–Sack formalism with the following 4×4 exchange matrix \mathbf{D}_2 .

$$\mathbf{D}_2 = \begin{array}{c} \begin{array}{cccc} \text{site} & \text{H}^\alpha\text{CN} & \text{H}^\beta\text{CN} & \text{CN}^- & [\text{Pd}(\text{CN})_4]^{2-} \\ \hline & -k_r^{\text{HCN}} & 0 & k_r^{\text{HCN}} & 0 \\ & 0 & -k_r^{\text{HCN}} & k_r^{\text{HCN}} & 0 \\ & (P^{\text{H}^\alpha\text{CN}}/2)k_r^{\text{HCN}} & (P^{\text{H}^\beta\text{CN}}/2)k_r^{\text{HCN}} & -(P^{\text{H}^\alpha\text{CN}}/P^{\text{CN}})k_r^{\text{HCN}} & (P^{\text{CN}^\text{b}}/P^{\text{CN}})k_r^{\text{Pd}} \\ & 0 & 0 & k_r^{\text{Pd}} & -k_r^{\text{Pd}} \end{array} \end{array} \quad (11)$$

\mathbf{D}_2 is composed of the three sites for the ligand (H^αCN , H^βCN , and CN^-) and one site for the complex $[\text{Pd}(\text{CN})_4]^{2-}$, with the corresponding populations $P^{\text{H}^\alpha\text{CN}}/2$, $P^{\text{H}^\beta\text{CN}}/2$, P^{CN} , and P^{CN^b} . The resonance frequencies of H^αCN , H^βCN , CN^- , and $[\text{Pd}(\text{CN})_4]^{2-}$ were fixed to 11 441, 11 169, 16 638, and 13 200 Hz, respectively, on a 400 MHz NMR spectrometer. The inverse of the mean lifetime of cyanide at the HCN site, k_r^{HCN} , was fixed at values calculated from activated parameters given previously. The inverse of the mean lifetime of cyanide at the $[\text{Pd}(\text{CN})_4]^{2-}$ site, k_r^{Pd} , was determined as a function of the free-cyanide concentration by fitting the experimental spectra. k_r^{Pd} is defined for the exchange of a particular cyanide on the metal center Pd(II). The observed kinetic rate constant of cyanide exchange on Pd(II), $k_{\text{obs}}^{\text{Pd,CN}}$ (eq 12), is given by k_r^{Pd} ($k_{\text{obs}}^{\text{Pd,CN}} = k_r^{\text{Pd}}$). The analysis of $[\text{CN}^-]$ dependence shows a negligible first-order $k_1^{\text{Pd,CN}}$ term, and a purely second-order rate law was fitted to the experimental data, leading to $k_2^{\text{Pd,CN}} = 78 \pm 2 \text{ s}^{-1} \text{ mol}^{-1} \text{ kg}$.

$$k_{\text{obs}}^{\text{Pd,CN}} = \frac{-d[\text{Pd}(\text{CN})_4^{2-}]}{dt [\text{Pd}(\text{CN})_4^{2-}]} = k_2^{\text{Pd,CN}} [\text{CN}^-] \quad (12)$$

(25) Fasman, A. B.; Kutuykov, G. C.; Sokolskii, D. V. *Zh. Neorg. Khim.* **1965**, *10*, 1338.

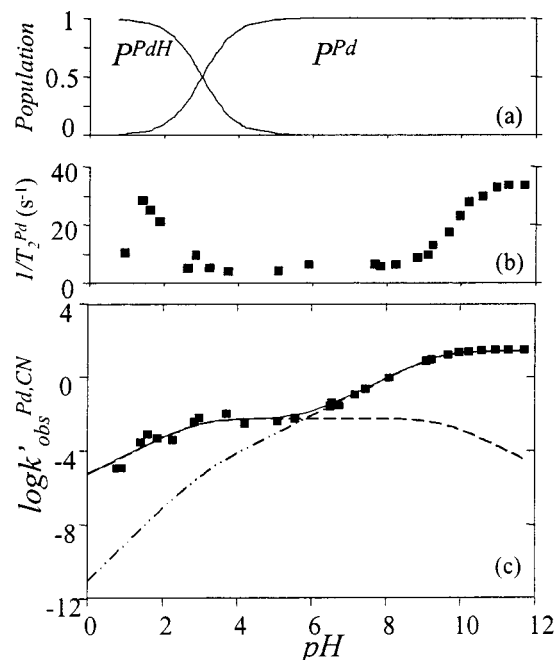


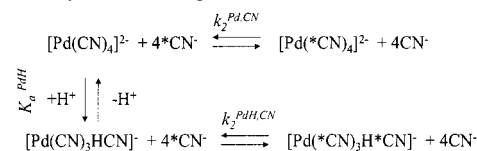
Figure 5. (a) Variation of the populations P^{Pd} of $[Pd(CN)_4]^{2-}$ and P^{PdH} of $[Pd(CN)_3(HCN)]^-$ with pH. (b) Evolution of the complex line width, $1/T_2^{Pd}$, as a function of pH. $C_{Pd} = 0.095 \text{ mol kg}^{-1}$ and $C_{CN} = 0.374 \text{ mol kg}^{-1}$. (c) Variation of the concentration-normalized ($C_{CN} = 0.4 \text{ mol kg}^{-1}$) rate constant $k'_{obs}^{Pd,CN}$ with pH for cyanide exchange on $[Pd(CN)_4]^{2-}$, with the contribution of both pathways. (---) $P^{Pd}k_2^{Pd,CN}[CN^-]$ and (- · - ·) $P^{PdH}k_2^{PdH,CN}[CN^-]$. $C_{Pd} = 0.095 \text{ mol kg}^{-1}$, $I = 0.66 \text{ mol kg}^{-1}$, and $D_2O/H_2O = 2\%$.

A variable-temperature study (287.3–328.9 K) of the exchange reaction was performed on a solution containing 0.1 mol kg^{-1} of the Pd complex and $0.472 \text{ mol kg}^{-1}$ of the free cyanide at pH = 11.4 by extracting the rate constants from the line-shape analysis of the ^{13}C NMR spectra. Higher temperatures could not be used without decomposition of the cyanide. The exchange rate constant at 298.1 K, $(k_2^{Pd,CN})^{298} = 88 \pm 3 \text{ s}^{-1} \text{ mol}^{-1} \text{ kg}$, and the activation parameters $\Delta H_2^\ddagger Pd,CN = 23.5 \pm 1.1 \text{ kJ mol}^{-1}$ and $\Delta S_2^\ddagger Pd,CN = -141.9 \pm 4.0 \text{ J mol}^{-1} \text{ K}^{-1}$ were obtained with an Eyring fit to the data.

A variable-pressure study at pH = 11.4 and 323.1 K was performed on a 0.1 mol kg^{-1} $[Pd(CN)_4]^{2-}$ solution containing $0.371 \text{ mol kg}^{-1}$ of the free ligand. The variation of $k_2^{Pd,CN}$ with pressure was calculated from the observed rate constant $k_{obs}^{Pd,CN}$, which was determined using the Kubo–Sack formalism (\mathbf{D}_2 matrix). The activation volume $\Delta V_2^\ddagger = -22 \pm 2 \text{ cm}^3 \text{ mol}^{-1}$ and the zero-pressure rate constant $(k_2^{Pd,CN})_0 = 197 \pm 15 \text{ s}^{-1} \text{ mol}^{-1} \text{ kg}$ were determined by fitting eq 11 to the variable-pressure data. The value of the compressibility coefficient of activation, $\Delta\beta^\ddagger = -(8 \pm 1) \times 10^{-2} \text{ cm}^3 \text{ mol}^{-1} \text{ MPa}^{-1}$, is noteworthy.

A variable-pH study gave us another opportunity to study how the rate law changes with C_{CN} concentration. The ^{13}C NMR spectra in Figure 1b were used to extract the observed rate constants, $k_{obs}^{Pd,CN}$, using the Kubo–Sack formalism with the \mathbf{D}_2 matrix in the basic domain (pH 11.7–9.1). Below pH 9, the rate constant was too small to induce detectable line-broadening in the signal of the coordinated CN^- . Thus, magnetization transfer experiments were performed from pH

Scheme 1. Cyanide Exchange on Pd(II) Center



8.1 to 6.5. Selective inversions were performed on the signal of the free or the bound ligand. Below pH 6, the exchange rate is slow compared to the longitudinal relaxation rate, and $k_{obs}^{Pd,CN}$ could not be determined using magnetization transfer. At pH ≤ 6.7 , the exchange rate was determined using isotopic labeling experiments. The isotopic labeling experiment was performed at pH = 6.7 (the highest value) to overlap with the domain where magnetization transfer techniques were applied. The value of rate constant does not vary with the modification of the technique. Twelve experiments were performed from pH 6.7 to 0.8 (Figure 5).

All observed rate constants are represented as a function of pH in Figure 5. In basic solution (pH > 10), $k_{obs}^{Pd,CN}$ is pH-independent. For pH < 10, $k_{obs}^{Pd,CN}$ decreases with pH because of the decrease in the concentration of CN^- upon protonation. The rates reach a second plateau between pH 6 and 3 and decrease again for pH < 3. Pd(II) behavior is different than that of Pt(II). This difference can be explained by the formation of a protonated complex whose influence on the observed rate constant can be deduced from Scheme 1.

The rate law (eq 13) is thus composed by two terms: $k_2^{Pd,CN}$, the second-order rate constant of cyanide exchange on $[Pd(CN)_4]^{2-}$, and $k_2^{PdH,CN}$, the second-order rate constant of cyanide exchange on the protonated complex $[Pd(CN)_3(HCN)]^-$. $K_a^{Pd(4,H)}$ and K_a^{HCN} are the proton dissociation constants of $[Pd(CN)_3(HCN)]^-$ and HCN, respectively.

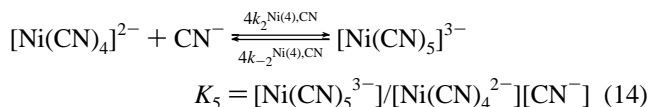
$$k_{obs}^{Pd,CN} = P^{Pd}k_2^{Pd,CN}[CN^-] + P^{PdH}k_2^{PdH,CN}[CN^-] = (P^{Pd}k_2^{Pd,CN} + P^{PdH}k_2^{PdH,CN}) \frac{K_a^{HCN}}{K_a^{HCN} + [H^+]} C_{CN} \quad (13)$$

$P^{Pd} = K_a^{Pd(4,H)} / (K_a^{Pd(4,H)} + [H^+])$ and $P^{PdH} = [H^+] / (K_a^{Pd(4,H)} + [H^+])$ are the populations of $[Pd(CN)_4]^{2-}$ and $[Pd(CN)_3(HCN)]^-$, respectively (Figure 5a). Equation 13 was fitted to the observed rate constants $k_{obs}^{Pd,CN}$ between pH 11.7 and 0.8, leading to the proton dissociation constant $K_a^{Pd(4,H)} = 3.0 \pm 0.3$ and to the second-order rate constants $k_2^{Pd,CN} = 67 \pm 13 \text{ s}^{-1} \text{ mol}^{-1} \text{ kg}$ and $k_2^{PdH,CN} = (4.5 \pm 1.3) \times 10^3 \text{ s}^{-1} \text{ mol}^{-1} \text{ kg}$ (Figure 5). The contributions of both pathways are shown in Figure 5c. The $k_{obs}^{Pd,CN}$ values were normalized with respect to concentration $C_{CN} = 0.4 \text{ mol kg}^{-1}$, leading to $k'_{obs}^{Pd,CN}$ values as a function of pH.

Cyanide Exchange on $[Ni(CN)_4]^{2-}$. The ionic strength was fixed with potassium triflate to avoid complex formation with the nitrate.²⁶ Two ^{13}C NMR signals are obtained if KNO_3 is added to a solution of $[Ni(CN)_4]^{2-}$. The overall formation constant of $[Ni(CN)_4]^{2-}$ (yellow) in aqueous solution has been determined by UV–visible and IR

(26) Beck, M.; Bjerrum, J. *Acta Chem. Scand.* **1962**, *16*, 2050.

spectroscopy and leads to a $\log \beta_4 = 30.3 \pm 0.1$.²⁷ At high CN^- concentration, a pentacoordinated $[Ni(CN)_5]^{3-}$ (red) species is formed, and the formation constant K_5 is small ($K_5 \approx 0.15 \text{ mol l}^{-1}$) and depends slightly on the ionic strength.²⁸



The $[Ni(CN)_4]^{2-}$ ion is very stable in water (nickel bis-(dimethyl)glyoximate, for instance, is soluble in aqueous cyanide solution). However, it is rapidly dissociated at $pH < 4$, with the formation of $Ni(CN)_2$ and finally Ni^{2+} .^{29–31} This process is reversible by adding KOH and raising the pH to 4. Before and during the dissociation process, $[Ni(CN)_4]^{2-}$ can be protonated. Margerum and Kolski²⁹ have measured the following three successive proton dissociation constants: $pK_a^{Ni(4,H)} = 5.4$ for $[Ni(CN)_3(HCN)]^-$, $pK_a^{Ni(4,2H)} = 4.5$ for $[Ni(CN)_2(HCN)_2]$, and $pK_a^{Ni(4,3H)} = 2.6$ for $[Ni(CN)(HCN)_3]^+$.

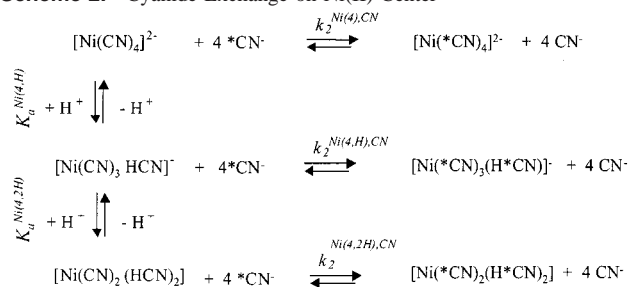
The cyanide exchange on $[Ni(CN)_4]^{2-}$ at very high pH is known to be fast on the NMR time scale, and previously only the limit⁸ ($> 5 \times 10^5 \text{ s}^{-1} \text{ mol kg}^{-1}$) of the exchange rate constant was given. The cyanide exchange induces line broadening over the entire pH domain (Figure 1c); therefore, the intermolecular-exchange rate constant can be extracted from line-shape analysis using the Kubo–Sack formalism from pH 10.3 to 3.8. At $pH > 7$, the exchange matrix must be modified relative to the palladium system to take into account the pentacoordinated species. The protonation of $[Ni(CN)_4]^{2-}$ can be neglected under these basic condition. The new exchange matrix D_3 is given in eq 15. It is composed of five sites: two for HCN, one for CN^- , one for the tetracyano complex, Ni(4), and one for the pentacyanonickelate(II), Ni(5), site.

sites	H^aCN	H^bCN	CN^-	Ni(4)	Ni(5)	population
$D_3 =$	$-k_r^{HCN}$	0	k_f^{HCN}	0	0	$p^{HCN/2}$
	0	$-k_r^{HCN}$	k_f^{HCN}	0	0	$p^{HCN/2}$
	$\frac{p^{HCN}}{2p^{CN}} k_r^{HCN}$	$\frac{p^{HCN}}{2p^{CN}} k_r^{HCN}$	$\frac{p^{HCN}}{4p^{CN}} k_r^{Ni(4)}$	0	$\frac{p^{Ni(4)}}{4p^{CN}} k_r^{Ni(4)}$	p^{CN}
	0	0	0	$-k_r^{Ni(4)}$	$k_f^{Ni(4)}$	$p^{Ni(4)}$
	0	0	$\frac{p^{Ni(4)}}{4p^{Ni(5)}} k_r^{Ni(4)}$	$\frac{p^{Ni(4)}}{p^{Ni(5)}} k_r^{Ni(4)}$	$-\frac{5p^{Ni(4)}}{4p^{Ni(5)}} k_r^{Ni(4)}$	$p^{Ni(5)}$

The value of the rate constant k_r^{HCN} is the same as that in the palladium D_2 matrix. The rate constant $k_r^{Ni(4)}$ is the inverse

- (27) Freund, H.; Schneider, C. R. *J. Am. Chem. Soc.* **1959**, *81*, 4780.
 (28) (a) Penneman, R. A.; Bain, R.; Gilbert, G.; Jones, L. H.; Nyholm, R. S.; Reddy, K. N. *J. Am. Chem. Soc.* **1963**, *85*, 6. (b) Van Geet, A. L.; Hume, D. N. *Inorg. Chem.* **1964**, *4*, 523. (c) Pierrard, J. C.; Hugel, R. *Rev. Chim. Miner.* **1971**, *8*, 831. (d) McCullough, R. L.; Jones, H. L.; Penneman, R. A. *J. Inorg. Nucl. Chem.* **1960**, *13*, 286.
 (29) Kolski, G. B.; Margerum, D. W. *Inorg. Chem.* **1968**, *7*, 2239.
 (30) Persson, H. *Acta Chem. Scand. A* **1974**, *28*, 885.
 (31) Persson, H.; Ekström, C. G. *Acta Chem. Scand., Ser. A* **1976**, *30*, 31.

Scheme 2. Cyanide Exchange on Ni(II) Center



of the mean lifetime of cyanide at the $[Ni(CN)_4]^{2-}$ site. According to this matrix, cyanide exchange takes place only via the formation of the pentacoordinated species. The resonance frequencies of H^aCN , H^bCN , CN^- , and $[Ni(CN)_4]^{2-}$ were fixed at 11 441, 11 169, 16 638, and 13 645 Hz, respectively, on a 400 MHz spectrometer. The populations were calculated as functions of the nickel concentration, C_{Ni} , the total cyanide concentration, C_{tot} ($C_{tot} = C_{CN} + 4C_{Ni}$), the formation constant of $[Ni(CN)_5]^{3-}$, K_5 (eq 15), the dissociation constant of HCN, K_a^{HCN} , and the pH.

To be able to use matrix D_3 , the resonance frequency of $[Ni(CN)_5]^{3-}$ was first determined. Six solutions were prepared at pH 11.4 with 0.05 mol kg^{-1} of $[Ni(CN)_4]^{2-}$ and variable amounts of KCN (0.06–0.52 mol kg^{-1}). The ^{13}C NMR spectra of these solutions showed a coalesced singlet that shifted downfield as the cyanide concentration increased. The resonance frequency of $[Ni(CN)_5]^{3-}$ can be deduced from the variation in the shift of the coalesced signal by fitting eq 16 as a function of C_{tot} to the ^{13}C data. δ_{CN} (165.1 ppm), $\delta_{Ni(4)}$ (135.6 ppm), and $\delta_{Ni(5)}$ are the resonance frequencies of cyanide in CN^- , $[Ni(CN)_4]^{2-}$, and $[Ni(CN)_5]^{3-}$, respectively.

$$\delta_{obs} = p^{CN} \delta_{CN} + 4p^{Ni(4)} \delta_{Ni(4)} + 5p^{Ni(5)} \delta_{Ni(5)} \quad (16)$$

The populations were calculated as functions of C_{tot} , C_{Ni} , K_5 , and pH. K_5 was fixed to the value found by Hugel, $0.168 \pm 0.003 \text{ mol}^{-1} \text{ kg}^{28c}$. A Lorentzian function was fitted to each spectrum, and the analysis of the dependence of the resonance frequency on the concentration of CN^- led to the adjusted resonance frequency of $\delta_{Ni(5)} = 230 \pm 26$ for $[Ni(CN)_5]^{3-}$.

pH Variation on $[Ni(CN)_4]^{2-}$. The rate of the cyanide exchange on $[Ni(CN)_4]^{2-}$ was determined as a function of pH. At basic pH, D_3 is used because of the formation of the pentacoordinated species. However, at low pH, the pentacoordinated complex can be neglected, but the protonated complexes must be taken into account. The cyanide exchange can take place via the three pathways given in Scheme 2:

Surprisingly, the protonation does not affect the chemical shift of the ^{13}C NMR complexed-cyanide signal. Therefore, the three complexes have the same $[Ni(CN)_4]^{2-}$ signal in ^{13}C NMR. For this reason, D_2 was used for $pH < 8$. The four sites correspond to H^aCN , H^bCN , CN^- , and $Ni(4)_{tot}$, the tetracoordinated complexes of Ni(II) with or without protonation. The observed rate constant of the cyanide exchange at low pH is equal to $k_r^{Ni(4)}$ in D_2 . This observed rate constant can be expressed as a function of the free-

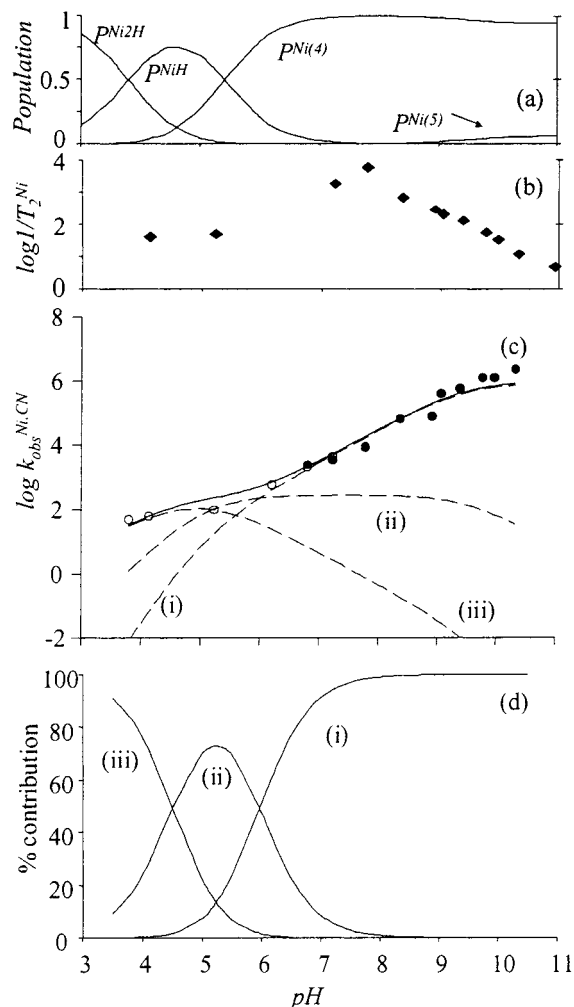


Figure 6. (a) Variation of the populations $P^{Ni(5)}$ of $[\text{Ni}(\text{CN})_5]^{3-}$, $P^{Ni(4)}$ of $[\text{Ni}(\text{CN})_4]^{2-}$, $P^{Ni(4,H)}$ of $[\text{Ni}(\text{CN})_3\text{HCN}]^-$, and $P^{Ni(4,2H)}$ of $[\text{Ni}(\text{CN})_2(\text{HCN})_2]$ with pH. (b) Evolution of the complex line width, $1/T_2^{\text{Ni}}$, as a function of pH. $C_{\text{Ni}} = 0.092 \text{ mol kg}^{-1}$ and $C_{\text{CN}} = 0.384 \text{ mol kg}^{-1}$. (c) Variation of the concentration-normalized ($C_{\text{CN}} = 0.4 \text{ mol kg}^{-1}$) rate constant $k_{\text{obs}}^{\text{Ni,CN}}$ with pH for cyanide exchange on $[\text{Ni}(\text{CN})_4]^{2-}$, with the contribution of three pathways: (i) $P^{Ni(4)}k_2^{\text{Ni(4),CN}}[\text{CN}^-] = P^{Ni(5)}k_{-2}^{\text{Ni(4),CN}}$, (ii) $P^{Ni(4,H)}k_2^{\text{Ni(4,H),CN}}[\text{CN}^-]$ for $k_2^{\text{Ni(4,H),CN}} = 10 \times 10^6 \text{ s}^{-1} \text{ mol}^{-1} \text{ kg}$, and (iii) $P^{Ni(4,2H)}k_2^{\text{Ni(4,2H),CN}}[\text{CN}^-]$. $C_{\text{Ni}} = 0.092 \text{ mol kg}^{-1}$, $I = 0.60 \text{ mol kg}^{-1}$, and $\text{D}_2\text{O}/\text{H}_2\text{O} = 2\%$.

cyanide concentration (eq 17).

$$k_{\text{obs}}^{\text{Ni,CN}} = (P^{Ni(4,2H)}k_2^{\text{Ni(4,2H),CN}} + P^{Ni(4,H)}k_2^{\text{Ni(4,H),CN}} + P^{Ni(4)}k_2^{\text{Ni(4),CN}}) \frac{[\text{CN}^-]}{P^{Ni(4,2H)} + P^{Ni(4,H)} + P^{Ni(4)}} \quad (17)$$

^{13}C NMR spectra were measured as a function of pH at 298.1 K for a solution containing $0.093 \text{ mol kg}^{-1}$ of $[\text{Ni}(\text{CN})_4]^{2-}$ and $0.384 \text{ mol kg}^{-1}$. Equation 17 was fitted to the values of $k_{\text{obs}}^{\text{Ni,CN}}$ obtained with D_3 for pH = 10.3–7 and with D_2 for pH = 8–3 (Figure 6). The iteration routine led to the following values: $k_2^{\text{Ni(4),CN}} = (2.7 \pm 0.4) \times 10^6 \text{ s}^{-1} \text{ mol}^{-1} \text{ kg}$, $k_2^{\text{Ni(4,H),CN}} < 10 \times 10^6 \text{ s}^{-1} \text{ mol}^{-1} \text{ kg}$, and $k_2^{\text{Ni(4,2H),CN}} = (50 \pm 18) \times 10^6 \text{ s}^{-1} \text{ mol}^{-1} \text{ kg}$. The populations were expressed as functions of C_{tot} , C_{Ni} , K_5 , $\text{p}K_{\text{a}}^{\text{HCN}}$, pH, $\text{p}K_{\text{a}}^{\text{Ni(4,H)}}$, and $\text{p}K_{\text{a}}^{\text{Ni(4,2H)}}$. Literature values of $\text{p}K_{\text{a}}^{\text{Ni(4,H)}}$ and $\text{p}K_{\text{a}}^{\text{Ni(4,2H)}}$ were used. We gave an upper limiting value to $k_2^{\text{Ni(4,H),CN}}$ because in the fitting procedure the $[\text{Ni}(\text{CN})_5(\text{HCN})]^-$

pathway can be suppressed without significantly affecting the values of the other two rate constants (Figure 6c and d).

Concentration Dependence. At pH = 7.5, cyanide exchange takes place predominately (more than 98%) via the $[\text{Ni}(\text{CN})_4]^{2-}$ complex. The cyanide exchange kinetics were determined as a function of the concentration of free cyanide to verify the rate law. At this pH, the presence of the protonated complexes could be neglected, but that of the protonated ligand could not (Figure 6a). Five solutions of $\text{K}_2[\text{Ni}(\text{CN})_4]$ (0.1 mol kg^{-1}) with variable KCN concentrations (0.059 – $0.952 \text{ mol kg}^{-1}$) were analyzed by ^{13}C NMR at 298.1 K. Using the Kubo–Sack formalism and D_2 , the $k_{\text{obs}}^{\text{Ni(4),CN}}$ values were extracted. They are linearly proportional to the concentration of the free- CN^- ligand (without the intercept) and lead to the second-order rate constant $k_2^{\text{Ni(4),CN}} = (2.5 \pm 0.5) \times 10^6 \text{ s}^{-1} \text{ mol}^{-1} \text{ kg}$. At pH = 3.8, the cyanide exchange (>85%) mainly occurs via the $[\text{Ni}(\text{CN})_2(\text{HCN})_2]$ species. Thus, the purely second-order rate law was also verified by measuring the rate constant as a function of the free-cyanide concentration. ^{13}C NMR spectra of five solutions containing 0.05 mol kg^{-1} of $\text{K}_2[\text{Ni}(\text{CN})_4]$ and 0.066 – $0.528 \text{ mol kg}^{-1}$ of KCN were obtained at 298.1 K, and rate constants were extracted from line-shape analysis using D_2 . The iteration volume led to the value $k_2^{\text{Ni(4,2H),CN}} = (67 \pm 4) \times 10^6 \text{ s}^{-1} \text{ mol}^{-1} \text{ kg}$ with a negligible first-order term. This value confirms that the value of $k_2^{\text{Ni(4,2H),CN}} = (50 \pm 18) \times 10^6 \text{ s}^{-1} \text{ mol}^{-1} \text{ kg}$ that was obtained with the pH-variation method is correct.

Temperature Dependence. A variable-temperature study of $k_{\text{obs}}^{\text{Ni,CN}}$ was performed at pH = 7.5 (and 272.1–323.1 K, mainly for $[\text{Ni}(\text{CN})_4]^{2-}$) and pH = 3.8 (and 274.6–329.8 K, mainly for $[\text{Ni}(\text{CN})_2(\text{HCN})_2]$) on solutions containing $0.100 \text{ mol kg}^{-1}$ of $\text{K}_2[\text{Ni}(\text{CN})_4]$ and $0.385 \pm 0.005 \text{ mol kg}^{-1}$ of KCN. Equation 9 was fitted to the values of $k_2^{\text{Ni(4),CN}}$ that were obtained at pH 7.5, leading to the following parameters: $(k_2^{\text{Ni(4),CN}})^{298} = (2.3 \pm 0.1) \times 10^6 \text{ s}^{-1} \text{ mol}^{-1} \text{ kg}$, $\Delta H_2^\ddagger_{\text{Ni(4),CN}} = 21.6 \pm 2 \text{ kJ mol}^{-1} \text{ kg}$, and $\Delta S_2^\ddagger_{\text{Ni(4),CN}} = -51 \pm 7 \text{ J mol}^{-1} \text{ kg K}^{-1}$. For the experiment at pH 3.8, we obtained the following parameters for the cyanide exchange on $[\text{Ni}(\text{CN})_2(\text{HCN})_2]$: $(k_2^{\text{Ni(4,2H),CN}})^{298} = (63 \pm 15) \times 10^6 \text{ s}^{-1} \text{ mol}^{-1} \text{ kg}$, $\Delta H_2^\ddagger_{\text{Ni(4,2H),CN}} = 47.3 \pm 1.0 \text{ kJ mol}^{-1} \text{ kg}$, and $\Delta S_2^\ddagger_{\text{Ni(4,2H),CN}} = 63 \pm 3 \text{ J mol}^{-1} \text{ kg K}^{-1}$.

Pressure Dependence. Variable-pressure ^{13}C NMR spectra were acquired at pH = 8.0 and $T = 297.5 \text{ K}$ for a solution containing $0.102 \text{ mol kg}^{-1}$ of $[\text{Ni}(\text{CN})_4]^{2-}$ and $0.382 \text{ mol kg}^{-1}$ of KCN. The rate constants $k_{\text{obs}}^{\text{Ni(4),CN}}$ were obtained using D_2 . These values give an the activation volume of $\Delta V_2^\ddagger_{\text{Ni(4),CN}} = -19 \pm 2 \text{ cm}^3 \text{ mol}^{-1}$, with a negligible compressibility coefficient of activation. Variable-pressure ^{13}C NMR experiments were also performed at pH = 3.5 and $T = 298.1 \text{ K}$ on a solution of 0.1 mol kg^{-1} of $\text{K}_2[\text{Ni}(\text{CN})_4]$ and $0.393 \text{ mol kg}^{-1}$ of KCN. An activation volume of $\Delta V_2^\ddagger_{\text{Ni(4,2H),CN}} = -6 \pm 1 \text{ cm}^3 \text{ mol}^{-1} \text{ kg}$ was calculated for the cyanide exchange on $[\text{Ni}(\text{CN})_2(\text{HCN})_2]$ at acidic pH.

Discussion

$[\text{M}(\text{CN})_4]^{2-}$ Complexes. The chemical shift data for the square-planar $[\text{M}(\text{CN})_4]^{2-}$ (Table 1) show a definitive trend

Table 1. ^{13}C NMR Chemical Shifts, $\log \beta_4$ Stability Constants, and F_{CN} and F_{MC} Force Constants of the $[M(\text{CN})_4]^{2-}$ Square-Planar Complexes

	δ (ppm)	$\log \beta_4$	F_{CN} (mdynes/Å)	F_{MC} (mdynes/Å)
CN^-	165.1		16.90 ^e	
$[\text{Ni}(\text{CN})_4]^{2-}$	135.5	31 ^a	17.20 ^f	2.25 ^f
$[\text{Pd}(\text{CN})_4]^{2-}$	131.2	51.7 ^b	17.44 ^f	2.32 ^f
$[\text{Pt}(\text{CN})_4]^{2-}$	125.0	40 ^c	17.41 ^f	2.75 ^f
HCN	112.4		18.70 ^e	
$[\text{Au}(\text{CN})_4]^-$	104.2	85 ^d	17.44 ^g	2.99 ^g

^a Reference 27. ^b Reference 25. ^c Reference 20. ^d Reference 36. ^e Reference 33. ^f Reference 34. ^g Reference 35.

to higher field as the progression from Ni(II) to Pd(II) to Pt(II) is made. The resonance frequency of the Au(III) complex lies at 104.2 ppm, which is below that of HCN and can be attributed to the higher charge of the metal center. A substantial shift to higher field was already observed for the ^{13}C resonance frequencies of isoelectronic cyano complexes as the metal oxidation state is increased.³² Another important factor affecting the chemical shift is the geometry of the cyano complex, which explains the high chemical shift value (230 ± 26 ppm) of the pentacyanonickelate(II) complex. In these complexes, the σ donation of the anionic CN^- likely dominates the π -backbonding; therefore, the variation of the chemical shift (from the shielding of the ^{13}C nucleus) also reflects the variation of the σ -bond strength: $\text{Au}-\text{C} > \text{Pt}-\text{C} > \text{Pd}-\text{C} > \text{Ni}-\text{C}$. The trend in the chemical shifts of the square-planar complexes is clearly observed for the $\text{M}-\text{C}$ force constants^{33–35} but is hardly observed for the $\text{C}-\text{N}$ force constants. These conclusions are consistent with the variation in $\log \beta_4$.³⁶

It is well-known that $[\text{Ni}(\text{CN})_4]^{2-}$ ($\text{p}K_{\text{a}}^{\text{Ni}(4,\text{H})} = 5.4$) can be protonated in acidic medium to form $[\text{Ni}(\text{CN})_3\text{HCN}]^-$ and further-protonated species.²⁹ Our kinetic results confirm this behavior and allow us, for the first time, to determine the $\text{p}K_{\text{a}}^{\text{Pd}(4,\text{H})}$ ($= 3.0 \pm 0.2$) of the palladium analogues kinetically. Surprisingly, for the palladium system, which undergoes slow intermolecular cyanide exchange at low pH, no variation of the chemical shift was observed with changes in pH, within experimental error. This result implies that resonance frequency variations due to protonation are small. Interestingly, the ^{13}C NMR line width of the bound cyanide at pH 3.5 increases slightly (from 1 to 10 Hz), in agreement with the $\text{p}K_{\text{a}}^{\text{Pd}(4,\text{H})}$ value determined from this work. A similar broadening is observed at pH 1.5 for the ^{13}C (from 2 to 7 Hz) and ^{195}Pt NMR signals (from 4 to 7 Hz) of the platinum complex. These observations are in line with the expected trend in $\text{p}K_{\text{a}}^{\text{M}(4,\text{H})}$ values: $\text{Ni} > \text{Pd} > \text{Pt}$.

Cyanide Exchange as a Function of pH. The $[\text{Pt}(\text{CN})_4]^{2-}$ complex has a purely second-order rate law, with CN^- acting as a nucleophile. Therefore, the observed exchange rate decreases ~ 9 orders of magnitude the pH decreases (Figure 7). The Pd(II) metal center exhibits similar behavior, with a

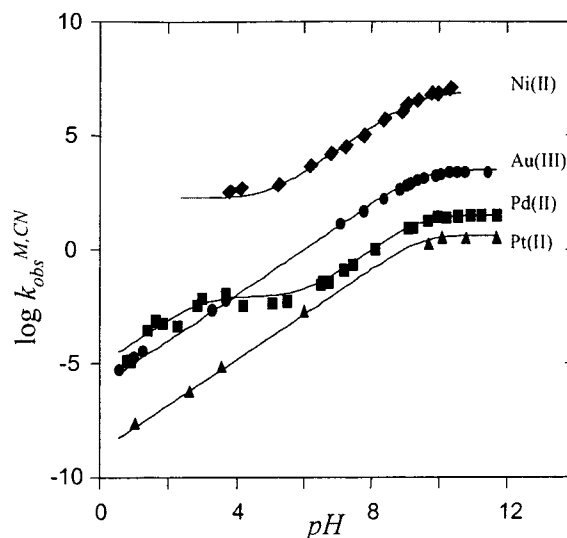


Figure 7. Variation of $k_{\text{obs}}^{\text{M,CN}}$ on $[M(\text{CN})_4]^{2-}$ in water at 298.1 K where $\text{M} = \text{Au}(\text{III}), \text{Pt}(\text{II}), \text{Pd}(\text{II}),$ and $\text{Ni}(\text{II})$. $C_{\text{CN}} = 0.4 \text{ mol kg}^{-1}$ and $C_{\text{M}} = 0.1 \text{ mol kg}^{-1}$.

decrease of ~ 4 orders of magnitude as the pH decreases to 6. At low pH, the tetracyanopalladate ($\text{p}K_{\text{a}}^{\text{Pd}(4,\text{H})} = 3.0 \pm 0.3$) is protonated to $[\text{Pd}(\text{CN})_3\text{HCN}]^-$. Because of a much faster cyanide exchange on $[\text{Pd}(\text{CN})_3\text{HCN}]^-$ ($k_2^{\text{Pd,H,CN}} \approx 55 k_2^{\text{Pd,CN}}$), the contribution of $[\text{Pd}(\text{CN})_3\text{HCN}]^-$ to the overall exchange becomes detectable around pH 6.5 and is predominant at $\text{pH} < 5.5$. The rate law of the cyanide exchange on the protonated complex is also purely second order. The $[\text{Ni}(\text{CN})_4]^{2-}$ is involved in various equilibrium reactions (formation of a pentacoordinated and of protonated complexes). At high pH, $[\text{Ni}(\text{CN})_4]^{2-}$ and $[\text{Ni}(\text{CN})_5]^{3-}$ are in equilibrium, as previously shown by UV–visible spectroscopy.^{27,28} Our ^{13}C NMR measurements have allowed to verify this behavior and to determine the rate constant ($k_2^{\text{Ni}(4,\text{CN})} = (2.3 \pm 0.1) \times 10^6 \text{ s}^{-1} \text{ mol}^{-1} \text{ kg}$) leading to the formation of $[\text{Ni}(\text{CN})_5]^{3-}$ as well as the backward rate constant ($k_{-2}^{\text{Ni}(4,\text{CN})} = 14 \times 10^6 \text{ s}^{-1}$). The overall CN^- exchange rate decreases down to pH 6, where the protonated complexes are formed. The reactivity of these complexes is higher because of protonation (Table 2). The rate law for $[\text{Ni}(\text{CN})_2(\text{HCN})_2]$ was found to be second order at pH 3.8.

For all cyanide exchanges on tetracyano complexes and on their mono- and diprotonated forms, we have always observed a pure second-order rate law: first order for the complex and first order for CN^- . However, this rate law does not apply to square-planar complexes. For example, the chloride exchange on $[\text{PtCl}_4]^{2-}$ takes place only via a reversible aqueous solvation process³⁷ (first-order rate law), but two pathways (first and second order) were observed for the chloride exchange on $[\text{AuCl}_4]^-$.³⁸ We set the following upper limits to the first-order terms of the cyanide exchange (from Figure 7): $> 10^{-9} \text{ s}^{-1}$ for Pt(II), 10^{-5} s^{-1} for Pd(II), and 10 s^{-1} for Ni(II). These limits imply that nucleophilic attack by HCN or solvation by H_2O for Pt(II), Pd(II), and Ni(II) is at least 9, 6, and 6 orders of magnitude

(32) Pesek, J. J.; Mason, W. R. *Inorg. Chem.* **1979**, *18*, 924 and references therein.

(33) Jones, L. H. *Inorg. Chem.* **1963**, *2*, 777.

(34) Kubas, G. J.; Jones, L. *Inorg. Chem.* **1974**, *13*, 2816.

(35) Jones, L. H.; Smith, J. M. *J. Chem. Phys.* **1964**, *41*, 2507.

(36) Remick, A. E. *J. Am. Chem. Soc.* **1947**, *69*, 94.

(37) Grantham, L. F.; Elleman, T. S.; Martin, D. S. *J. Am. Chem. Soc.* **1955**, *77*, 2965.

(38) Rich, R.; Taube, H. *J. Phys. Chem.* **1954**, *58*, 1.

Table 2. Activation Parameters of the Cyanide Exchange on the $[M(CN)_4]^{n-}/HCN/CN^-$ System in an Aqueous Medium at 298.1 K

metal		$k_2^{M,X}$ ($s^{-1} mol^{-1} kg^a$)	ΔH^\ddagger (kJ mol^{-1})	ΔS^\ddagger (J mol^{-1} K^{-1})	ΔV^\ddagger (cm^3 mol^{-1})
Ni(II) ^b	$k_2^{Ni(4),CN}$	$(2.3 \pm 0.1) \times 10^6$	21.6 ± 2	-51 ± 7	-19 ± 2
	$k_2^{Ni(4,H),CN}$	$< 10 \times 10^6$			
Pd(II) ^c	$k_2^{Pd(4),CN}$	$(63 \pm 15) \times 10^6$	47.3 ± 1	$+63 \pm 3$	-6 ± 1
	$k_2^{Pd(H),CN}$	82 ± 2^d	23.5 ± 1^d	-129 ± 5^d	-22 ± 2
Pt(II) ^e	$k_2^{Pt,CN}$	$(4.5 \pm 1.3) \times 10^3$			
Au(III) ^{e,f}	$k_2^{Pt,CN}$	11 ± 1^d	25.1 ± 1^d	-142 ± 4^d	-27 ± 2
	$k_2^{Au,CN}$	6240 ± 85	40.0 ± 1	-38 ± 3	$+2 \pm 1$
	$k_2^{Au,Cl}$	0.56 ± 0.03	65.1 ± 1	-31 ± 3	-14 ± 2

^a The rate constants reported are for the exchange of a particular coordinated X^- . The rate constant for an unspecified X^- is therefore four times greater than the rate constant for the coordinated X^- , and the corresponding ΔS^\ddagger value is 11.5 ($= R \ln 4$) times greater than ΔS^\ddagger for the coordinated X^- . ^b The rate law is given in equation 17. ^c The rate law is given in equation 13. ^d The kinetic parameters obtained previously for pH = 10.3 and 10.8 are for Pd (Pt): $k_2^{Pd,CN} = 124(25) s^{-1} mol^{-1} kg$; $\Delta H^\ddagger = 17(24) kJ mol^{-1}$, and $\Delta S^\ddagger = -147(137) J mol^{-1} K^{-1}$ from references 8 and 42. ^e $k_{obs}^{M,L} = k_2^{M,L} [L]$. ^f Reference 2.

slower, respectively, than nucleophilic attack by CN^- on Pt(II), Pd(II) and Ni(II), respectively.

We have recently reported the rate law and the pH variation of the cyanide exchange on Au(III) square-planar complex in water.² The observed cyanide-exchange rate constant on $[Au(CN)_4]^-$, $k_{obs}^{Au,CN}$, is also presented in Figure 7. The Au(III) and Pt(II) complexes are not kinetically affected by the protonation of the complex, whereas Pd(II) and Ni(II) show an important change at low pH because of the faster cyanide exchange on the protonated species. The increase of the rate at low pH can be attributed to the more positive charge of the protonated complex and to a weaker M-CN bond. No kinetic effect of the protonation of $[Pt(CN)_4]^{2-}$ is observed, probably because of a lower $pK_a^{Pt(4,H)}$ value, as discussed above.

Kinetic Parameters. All the activation parameters, rate constants, and rate laws are listed in Table 2. The cyanide-exchange rate constant on $[M(CN)_4]^{2-}$ increases in a 1:7:200 000 ratio for Pt/Pd/Ni (Figure 7). This trend is modified at low pH; the palladium becomes 400 times more reactive than the platinum because of the formation of $[Pd(CN)_3HCN]^-$. The high reactivity of $[Ni(CN)_4]^{2-}$ is explained by the stability of the pentacoordinate intermediate that becomes stable for nickel. $[Ni(CN)_5]^{3-}$ has been isolated with both regular square-pyramidal and distorted trigonal-bipyramidal geometries present in the same crystal.³⁹ The high reactivity of Au(III) with respect to the isoelectronic Pt(II) is explained by the higher oxidation state. The relative reactivity of palladium with respect to platinum depends strongly on the nature of the ligand involved in ligand exchange on their homoleptic complexes. The values of $k_2^{Pd,L}/k_2^{Pt,L}$ for H_2O , Me_2S , and $MeNC$ are 1.4×10^6 , 1.39×10^3 , and 1.7, respectively.^{40–44} $k_2^{Pd,L}/k_2^{Pt,L} = 7$ for CN^- exchange is of the

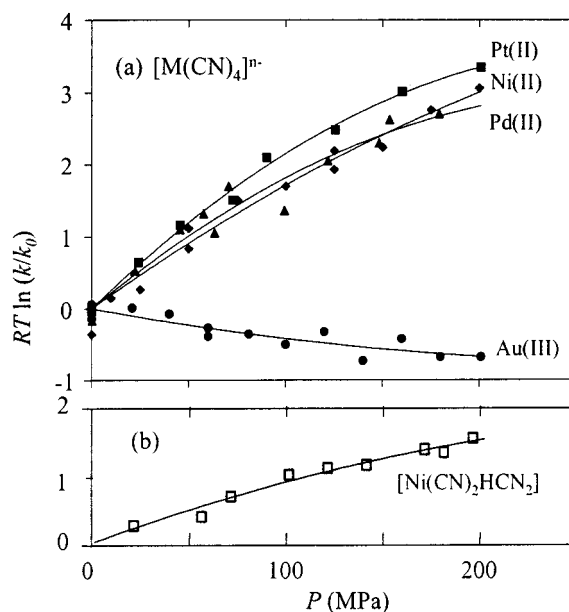


Figure 8. Effect of pressure on $RT \ln(k/k_{20})$ for the cyanide exchange (a) on $[M(CN)_4]^{n-}$ where $M = Au(III), Pt(II), Pd(II), and Ni(II)$, $C_M = 0.10 \pm 0.05 mol kg^{-1}$, $C_{CN} = 0.40 \pm 0.5 mol kg^{-1}$, and $I = 0.6 \pm 0.1 mol kg^{-1}$. For Au(III) and Pt(II), pH = 11.5, $T = 298.1 K$. For Pd(II), pH = 11.4 and $T = 323.1 K$. For Ni(II), pH = 10.4 and $T = 279.9 K$ and (b) on $[Ni(CN)_2(HCN)_2]$. $C_M = 0.10 \pm 0.05 mol kg^{-1}$, $C_{CN} = 0.40 \pm 0.5 mol kg^{-1}$, $I = 0.6 \pm 0.1 mol kg^{-1}$, pH = 3.5, and $T = 298.1 K$.

same order of magnitude as the value obtained for the isonitrile ligand and confirms the much higher selectivity of the Pt(II) center with respect to the Pd(II) center. The divalent complexes $[Ni(CN)_4]^{2-}$, $[Pd(CN)_4]^{2-}$, and $[Pt(CN)_4]^{2-}$ have approximately the same activation enthalpy; however, the difference in reactivity among these three complexes is reflected in the entropy term. The negative values of ΔS^\ddagger are indicative of an associative activation mode. The most negative values are observed for platinum and palladium, implying the formation of a fully pentacoordinated species at the transition state. The much less negative value for Ni(II) indicates that the coordination of the transition-state species is intermediate between tetra- and pentacoordination, as confirmed by the true thermodynamic equilibrium between $[Ni(CN)_4]^{2-}$ and $[Ni(CN)_5]^{3-}$.

Variable Pressure. The activation volumes are clearly negative and show the same trend as do the entropies (Table 2, Figure 8). Using the same argument as above and taking into account the fact that the pentacoordinated species is observed for nickel, we conclude that this species participates in a limiting A exchange pathway. We observed that the magnitude of the activation volume for cyanide exchange on Pd(II) is always smaller than that for the corresponding exchange on Pt(II).⁴² Furthermore, the ΔV^\ddagger values for CN^- exchange on $[Pt(CN)_4]^{2-}$ ($-27 cm^3 mol^{-1}$) and $[Pd(CN)_4]^{2-}$ ($-22 cm^3 mol^{-1}$) are the most negative ever observed for homoleptic square-planar ligand-exchange reactions. For example, the following ΔV^\ddagger values were reported for Pt(II) and Pd(II), respectively, in Me_2S and in H_2O : -22 and -9.4

(39) (a) Raymond, K. N.; Corfield, P. W. R.; Ibers, J. A. *Inorg. Chem.* **1968**, *7*, 1362. (b) Jurnak, F. A.; Raymond, K. N. *Inorg. Chem.* **1974**, *13*, 2387.

(40) Helm, L.; Elding, L. I.; Merbach, A. E. *Inorg. Chem.* **1985**, *24*, 1719.

(41) Helm, L.; Elding, L. I.; Merbach, A. E. *Helv. Chim. Acta* **1984**, *67*, 1453.

(42) Frey, U.; Elmroth, S.; Moullet, B.; Elding, L.; Merbach, A. E. *Inorg. Chem.* **1991**, *30*, 5033.

(43) Olsson, A.; Kofod, P. *Inorg. Chem.* **1992**, *31*, 183.

(44) Hallinan, N.; Besançon, V.; Forster, M.; Elbaze, G.; Ducommun, Y.; Merbach, A. E. *Inorg. Chem.* **1991**, *30*, 1112.

Cyanide Exchange on $[M(CN)_4]^{2-}$

$\text{cm}^3 \text{ mol}^{-1}$ (Me_2S) and -4.6 and $-2.2 \text{ cm}^3 \text{ mol}^{-1}$ (H_2O). Therefore, we attribute our results to a limiting A mechanism, even though an intermediate could not be formally detected. The ΔV^\ddagger value for cyanide exchange on $[\text{Ni}(\text{CN})_2(\text{HCN})_2]$ is much less negative than that for the deprotonated species, but the value for the entropy of cyanide exchange on $[\text{Ni}(\text{CN})_2(\text{HCN})_2]$ is less positive than that for the deprotonated species. These results are indicative of a type I/I_a interchange process with a small amount of associative character.

Conclusions

The cyanide exchange on $[M(\text{CN})_4]^{2-}$ with $M = \text{Pt}, \text{Pd}$, and Ni is a rare case in which mechanistic comparisons between 3d, 4d, and 5d transition-metal complexes. Surprisingly, the behavior of these metal square-planar centers leads to mechanistic diversity involving pentacoordinated species

or transition states as well as protonated complexes. The reactivities of these species are strongly pH-dependent, covering 15 orders of magnitude in reaction rates. The nucleophilic attack by HCN is at least 6–9 orders of magnitude slower than is the nucleophilic attack by CN^- on $[M(\text{CN})_4]^{2-}$.

Acknowledgment. We thank the Swiss National Science Foundation for financial support.

Supporting Information Available: All exchange rate constants as a function of pH, concentration, temperature, and pressure; tables of the resonance frequencies and line widths; fitted parameters for magnetization transfer and isotopic labeling experiments. This material is available free of charge via the Internet at <http://pubs.acs.org>.

IC010917E